

# ADAPTIVE REAL-TIME CARDIAC MRI USING *PARADISE*: VALIDATION BY THE PHYSIOLOGICALLY IMPROVED NCAT PHANTOM

Behzad Sharif and Yoram Bresler

Department of Electrical and Computer Engineering, Coordinated Science Laboratory University of Illinois, Urbana-Champaign, IL, USA

## Abstract

Patient-Adaptive Reconstruction and Acquisition Dynamic Imaging with Sensitivity Encoding (*PARADISE*) is a dynamic MR imaging scheme that optimally combines parallel imaging and model-based adaptive acquisition. In this work, we propose the application of *PARADISE* to real-time cardiac MRI. We introduce a physiologically improved version of a realistic four-dimensional cardiac-torso (NCAT) phantom, which incorporates natural beat-to-beat heart rate and motion variations. Cardiac cine imaging using *PARADISE* is simulated and its performance is analyzed by virtue of the improved phantom. Results verify the effectiveness of *PARADISE* for high resolution un-gated real-time cardiac MRI and its superiority over conventional acquisition methods.

## Index Terms

Dynamic MRI; Adaptive Acquisition; Cardiac Phantom; Real-time Cardiac Imaging; Time-Sequential Sampling

## 1. INTRODUCTION

Dynamic magnetic resonance (MR) imaging involves reconstruction of a dynamic object from samples of its spatial Fourier transform. For any dynamic imaging scheme, the sampling strategy, which defines the acquisition procedure, is subject to an inherent time-sequential (TS) sampling constraint: only limited data in  $k$ -space (spatial Fourier domain) can be acquired at any one time. Owing to limited speed of MR acquisition, even with the fastest pulse sequences, it is infeasible to sample the entire  $k$ -space at the required Nyquist rate.

As an instance of dynamic imaging, cardiac MR (CMR) imaging, suffers from the same acquisition speed limitation addressed above. The typical resolution in CMR is to attempt to “freeze” cardiac motion through ECG-gating and breath-holding. However these methods can only provide a static view of the dynamic process time-averaged over several cardiac cycles. Moreover, cardiac function exhibits natural beat-to-beat variability even in healthy humans and averaging such variability over time results in inaccurate images. Besides, gated techniques are incapable of imaging transient cardiac phenomena present in certain pathologies and are completely ineffective in patients with some form of arrhythmia. Therefore, it is necessary to develop methods for acquiring CMR images in the presence of physiological motion, e.g. beating heart or blood flow, while maintaining high resolution and good image quality.

The Patient-Adaptive Reconstruction and Acquisition Dynamic Imaging Method (PARADIGM) [1, 2] overcomes this limitation by adapting the MR data acquisition and the reconstruction to the spatial and temporal characteristics of the imaged object. Instead of attempting to freeze all motion by sufficiently fast acquisition, PARADIGM explicitly accounts for time variation during acquisition. This is achieved by using adaptive minimally-redundant acquisition and reconstruction procedures, which are automatically optimized for the specific object being imaged. The approach builds upon optimum time-sequential sampling theory [3, 4] but does not take advantage of parallel imaging hardware.

Parallel MRI techniques such as SENSE [5] or GRAPPA present a complementary hardware approach to accelerate the imaging process by using multiple receiver coils, with distinct spatial sensitivities, to simultaneously acquire  $k$ -space samples. This reduces the effective field-of-view (FOV) for data acquired by each coil and thus reduces the  $k$ -space Nyquist sampling rate requirement.

Based on the theory of multi-channel TS sampling theory, we proposed a parallel adaptive imaging scheme [6] which enables the acquisition to be accelerated by both model-based adaptive imaging as well as parallel imaging gaining up to the product of the individual accelerations. It produces an artifact-free reconstruction of the dynamic object for cases where artifact-free imaging with either parallel imaging or adaptive acquisition alone is infeasible. In this work, we study the application of this scheme, referred to as the Patient-Adaptive Reconstruction and Acquisition Dynamic Imaging with Sensitivity Encoding (PARADISE) method, to real-time CMR imaging. In the context of CMR, PARADISE is an un-gated real-time imaging technique that reconstructs a cardiac cine from MR data acquired without ECG triggering. It optimally adapts CMR data acquisition and cine reconstruction to both the cardiac model and to receiver coil sensitivities and achieves artifact-free real-time cardiac imaging while providing performance guarantees on achievable signal-to-noise ratio (SNR) and spatial- and temporal-resolutions. It also accommodates beat-to-beat variations in both heart rate and cardiac motion.

The objective of the present work is to validate the PARADISE scheme for CMR imaging applications, and evaluate its performance quantitatively by a realistic simulation study. As the tool to achieve these goals, we introduce a Physiologically-Improved NCAT (PIN-CAT) phantom based on the previously proposed NCAT computer phantom [7] which is a numerical spatial and temporal (4-D) cardiac-torso phantom extensively used for CT/PET studies. The improved phantom allows variation of anatomical and physiological parameters to simulate different disease states to test the robustness of an imaging scheme. Using the phantom we simulate a realistic CMR scenario. Because the exact anatomy and physiological functions of the phantom are known, this provides a gold standard by which to evaluate the imaging technique and compare it to other methods.

The paper is organized as follows. Section 2 introduces the proposed PINCAT phantom. In Section 3, we briefly describe the banded spatio-temporal model for the heart and present an overview of the theory underlying PARADISE. Section 4 describes the numerical experiments and discusses the results.

## 2. PHYSIOLOGICALLY IMPROVED NCAT PHANTOM

Cardiovascular variables such as heart rate (HR), arterial blood pressure, stroke volume and the shape of electrocardiographic complexes all vary beat-by-beat [8]. These further interact with respiration. This variability reflects the dynamic response of the cardiovascular (CV) regulatory systems to perturbations in the CV function. Because of the difficulty to control and isolate these physiological variability effects, and their complex interaction with the

specific pulse sequence and imaging protocol, it is difficult to study their effects on image accuracy and quality in-vivo. Instead, we propose the use of a versatile and physiologically realistic phantom.

The four-dimensional (spatial and temporal) nonuniform rational B-spline based Cardiac-Torso (NCAT) phantom [7] was developed to provide an accurate and flexible model of human anatomy and physiology. It includes a realistic model for the cardiac and respiratory motions based on tagged MRI data and respiratory-gated CT data respectively. The NCAT phantom models the main coronary arteries based on 3D angiogram data and also cardiac twisting and lateral motions. The NCAT phantom allows specifications of anatomic and physiological parameters such as HR, respiratory rate, LV volume etc. Combined with models of the imaging process, the NCAT phantom is used to generate simulated imaging data and reconstructions. The tissue contrast parameters in the NCAT phantom were modified for MR imaging applications. Note that this contrast depends on the MR pulse sequence and the sequence parameters. With this modification, the NCAT phantom can be used to simulate cardiac MR imaging applications. However, the NCAT phantom assumes periodic cardiac and respiratory motions which are not physiologically realistic especially for cardiac-compromised subjects.

We propose to combine the MR NCAT phantom with the Research CV Simulator [8] that models the beat-to-beat variation in morphology and timing of the human CV system. The model is based on an extensive list of heart and circulatory parameters that characterize the intact circulation. The proposed Physiologically Improved NCAT (PINCAT) phantom post-processes the NCAT-generated image sequence such that it matches the beat-to-beat changes predicted by the CV simulator. The processing ensures that we match (1) the cardiac aperiodicity modeled due to the various physiological effects including hemodynamic response to respiration and baroreflex control; (2) beat-to-beat variation in cardiac motion reflected for instance in changes in end-diastolic volume from beat-to-beat. This is achieved by appropriate processing of the image sequence generated by the NCAT phantom and time-warping the resulting sequence where the time-warp function is computed according to the instantaneous HR provided by the CV simulator. Although in this work we use the PINCAT phantom to evaluate the PARADISE scheme, the proposed phantom is useful for evaluating other cardiac MR data acquisition and reconstruction methods as well.

### 3. CARDIAC MRI WITH PARADISE

The time-varying object with  $d$ -spatial dimensions is denoted by  $I(r, \vec{t})$ ,  $r \in \mathbb{R}^d$ . Fourier transforms (FT) of signals are indicated by the variables used, e.g.,  $I(k, f)$  is the Fourier transform of  $I(r, \vec{t})$  w.r.t.  $r$  and  $t$ ;  $k$  and  $f$  refer to the spatial and temporal frequencies respectively.

#### 3.1. A Banded Spectral Model of the Heart for Dynamic MRI

The banded spectral model [2, 3], characterizes the cardiac object,  $I(r, \vec{t})$ , by its support  $B = \text{supp}\{I(r, \vec{t})\}$  in the dual  $k$ - $t$  (DKT) space, i.e., the  $x$ - $y$ - $f$  space, as shown in Fig. 1(a). This model captures (1) the finite spatial FOV outside which the function is zero, (2) the approximate periodicity of the cardiac motion reflected in the quasi-harmonic banded temporal spectrum with frequency spacing determined by the HR, and (3) the spatial localization of the fast motion to the heart-region defining the dynamic field-of-view. The specific parameters for the model differ among subjects depending on their HR, HR variability and heart position, and is robustly estimated using a pilot MR scan [2].

In order to illustrate the effect of beat-to-beat motion variability, in Fig. 1(b) we have shown a 1-D profile through the DKT support of (1) periodic NCAT phantom (2) PINCAT

phantom with HR and motion variability. The spectra are calculated from a 20 second short-axis heart movie. Because of the finite time window, even in the exactly periodic case the harmonics have finite, non-zero bandwidth. As expected [2], the figure demonstrates that the harmonic bands are widened due to beat-to-beat variations in the cardiac function.

### 3.2. PARADISE Theory and Algorithm

Given  $L$  receiver channels, the imaging equation in parallel MRI is:

$$D_\ell(\vec{k}, t) = \int_{FOV} s_\ell(\vec{r}) I(\vec{r}, t) e^{-i2\pi \vec{k} \cdot \vec{r}} d\vec{r} \quad (1)$$

where  $\{s_\ell(\vec{r})\}_{\ell=1}^L$  are the time-invariant coil sensitivities. We consider Cartesian 2-D Fourier imaging, i.e.,  $\vec{r} = \begin{bmatrix} x & y \end{bmatrix}$ , with slice selection along the  $z$  direction and  $k_x$  as the readout direction. Acquisition along the readout direction is sufficiently fast to be assumed instantaneous relative to the cardiac dynamics. Consequently, we have a 2-D sampling problem in the  $(k_y, t)$  domain where each point corresponds to a horizontal line in  $(k_x, k_y)$ . Due to the TS constraint only one line can be acquired at each time instance. Consider a temporally-uniform TS sampling lattice  $\Lambda$  with basis matrix  $\mathbf{A}$ . According to multi-dimensional sampling theory, sampling on  $\Lambda$  in  $(k_y, t)$  will result in replications of the spectrum in the DKT domain, i.e.  $(y, f)$ . Figure 2 demonstrates the effect in the DKT domain which in general results in overlaps over the object's DKT support  $\mathcal{B}$ . Sampling  $D_\ell(k_y, t)$  on  $\Lambda$  in  $(k_y, t)$  and taking the inverse FT in  $k_y$  and forward FT in  $t$  of the  $\ell$ -th coil measurement, we arrive at:

$$d_\ell(y, f) = \frac{1}{|\det(\mathbf{A})|} \sum_{\vec{n} \in \mathbb{Z}^2} s_\ell\left(\begin{bmatrix} y \\ f \end{bmatrix} - \mathbf{A}^* \vec{n}\right) I\left(\begin{bmatrix} y \\ f \end{bmatrix} - \mathbf{A}^* \vec{n}\right) \quad (2)$$

where  $\mathbf{A}^* = \mathbf{A}^{-T}$  is the basis matrix for the polar lattice  $\Lambda^*$ . For a point  $(y_0, f_0) \in \mathcal{B}$ , define

$$\mathcal{Q}(y_0, f_0) = \left\{ \begin{bmatrix} y \\ f \end{bmatrix} \in \mathcal{B} \mid \exists \vec{n} \in \mathbb{Z}^2 \text{ s.t. } \begin{bmatrix} y \\ f \end{bmatrix} = \begin{bmatrix} y_0 \\ f_0 \end{bmatrix} - \mathbf{A}^* \vec{n} \in \mathcal{B} \right\}$$

to which we refer as the equivalence class (EC) of  $(y_0, f_0)$ . From (2), it follows that for a fixed  $(y_0, f_0) \in \mathcal{B}$ , the set  $\mathcal{Q}(y_0, f_0)$  contains all the points in  $\mathcal{B}$  that are aliasing with  $(y_0, f_0)$ . Figure 2 illustrates this where the two ends of the arrow mark members of an EC. It can be shown that the set of all ECs provides a partitioning of the  $(y, f)$  space. Now, for a fixed EC  $\mathcal{Q}(y_0, f_0)$  with a representative member  $(y_0, f_0) \in \mathcal{B}$ , (2) can be written in matrix form as follows:

$$\vec{d}(y_0, f_0) = \mathbf{S}(y_0, f_0) \vec{I}(y_0, f_0) \quad (3)$$

where  $\vec{d}(y_0, f_0)$  is a length- $L$  vector, containing the coil outputs for  $\ell = 1, \dots, L$ ,  $\vec{I}(y_0, f_0)$  contains the set of unknowns at locations  $(y, f) \in \mathcal{Q}(y_0, f_0)$ , and  $\mathbf{S}(y_0, f_0)$  is the forward matrix consisting of coil sensitivities. Given the MRI data,  $\vec{d}(y_0, f_0)$  is known for all  $(y_0, f_0) \in \mathcal{B}$  and solving the inverse problem in (3) will recover the main replica of the spectrum for all members of  $\mathcal{Q}(y_0, f_0)$ . Doing so for all ECs will give a reconstruction of the object in the  $(y, f)$  domain. If all of the ECs for a lattice  $\Lambda$  and support  $\mathcal{B}$  satisfy the necessary and sufficient reconstructability condition [6], we call that lattice “ $\mathcal{B}$ -unfoldable.” Since the coil measurements are corrupted by additive noise, a regularized linear minimum variance

estimator is used to solve (3) where the noise covariance matrix is estimated from the MR data. Subsequently,  $\hat{I}(y, t)$  is reconstructed by an inverse FT along  $f$ . For a 2-D object, this procedure can be repeated for all  $k_x$  to recover the whole object.

The PARADISE sampling design algorithm searches over all  $\mathcal{B}$ -unfoldable lattices [6] and finds the one that achieves or exceeds a predetermined acceleration factor while optimizing a predefined optimization criterion. In this work, we optimize the resulting SNR over the dynamic FOV by minimizing the following functional:

$$\bar{\varepsilon}(\Lambda, \mathcal{B}, \{s_\ell\}_{\ell=1}^L) = \|\vec{I} - \widehat{I}\|_2^2 = \sum_{p=1}^c \text{trace}\{(\mathbf{S}_p^H \Phi_n^{-1} \mathbf{S}_p)^{-1}\} \quad (4)$$

where  $\{\mathcal{Q}_p\}_{p=1}^c$  are the ECs covering the dynamic FOV,  $\mathbf{S}_p$  is the corresponding  $\mathbf{S}$  matrix for the class  $\mathcal{Q}_p$ , and  $\Phi_n$  is the noise covariance matrix. This procedure is similar to optimizing the geometric factor (g-factor) associated with parallel MRI [5]. In contrast to the PARADIGM scheme where no aliasing is allowed in the DKT domain, PARADISE, by virtue of its unaliasing capability, can handle denser sampling patterns in the  $(y, f)$  domain, i.e., lower sampling rates in  $(k_y, t)$  domain are achievable. Reconstructability conditions and limitations are discussed in [6].

## 4. RESULTS

A 4-D cardiac cine corresponding to a supine male patient was generated using the NCAT phantom with MR-adjusted contrast (bright blood imaging). In order to realistically simulate a breath-hold imaging experiment, a small respiratory drift was included in the cine by appropriately adjusting the NCAT phantom parameters. Next, the doubly-oblique short-axis slices were extracted and resized to a  $128 \times 128$  image matrix size. The cine was processed according to the CV simulator output to generate the PINCAT phantom as described in Section 2. It exhibited a HR range of 60–70 beats per minute and a maximum of 10% ventricular volume variability. The DKT support of the dynamic phantom was computed (plotted in solid line in Fig. 1(b)) and 95.2% of the energy (in the  $\ell_2$  sense) was captured by the first 10 harmonic bands each of width  $\Delta f = 0.27$  Hz. The dynamic region was assumed to occupy 40% of the FOV along the  $y$  direction. The MR scanner was assumed to have 8 receiver channels and the coil profiles were obtained using numerical simulation of Bio-Savart's law for a spherical water phantom. An SNR of 35dB was simulated by adding independent white Gaussian noise to the parallel coil outputs.

For the described scenario, the PARADIGM method, i.e., patient-adaptive acquisition with a single channel, requires a sampling interval (repetition time) of  $\text{TR}=2.84$  milliseconds (ms). In this experiment, we assumed a minimum feasible TR of 5.5 ms. Hence a minimum acceleration of  $R=1.94$  was required to achieve the spatial and temporal resolution targets. The PARADISE acquisition algorithm was run with these requirements while optimizing the resulting SNR performance. The optimal TS sampling pattern was computed which had a  $\text{TR}=5.625$  ms, i.e., acceleration of  $R=1.98$  over PARADIGM. Using the PINCAT-generated 2-D short-axis slice, data for this sampling pattern was generated for a total acquisition time of about 20s. Figure 3(b) shows a single frame from the reconstructed cine corresponding to the systolic phase of the heart along with the true PIN-CAT phantom frame shown in panel (a).

For comparison, we used a non-adaptive progressive acquisition scheme that sequentially acquires adjacent  $k$ -space lines, repeating the acquisition in a loop, and uses the sliding window method (in  $k$ - $t$  space) for reconstruction. To meet the desired resolution goals, this sampling scheme requires a TR of 0.372 ms which is infeasible for modern MR scanners.

This scheme can be accelerated by subsampling similar to the SENSE method [5]. However, to meet the TR limitations, the progressive scheme needs an acceleration factor of more than  $R=14$  which is infeasible with 8 receiver channels. Note that in practice, SENSE accelerations of more than half the number of coils is rarely attempted because of the high noise amplification due to the resulting g-factors [5]. In this experiment, for the progressive scheme, we used  $R=2$  with the minimum available TR of 5.5 ms. Figure 3(c) shows a single frame of the reconstructed cine.

Comparing the reconstructed frames to the ground truth in Fig. 3(a), it is seen that the two schemes have comparable SNR over the dynamic region but PARADISE uses the object model to filter out high-frequency noise in the static regions of the image, significantly improving the SNR in those regions. More importantly, although the PARADISE reconstruction is visually artifact-free, the progressive reconstruction shows the wrong cardiac phase (the diameter of the left ventricle is too large). In other words, temporal resolution of the progressive scheme is insufficient to capture the true dynamics of the heart. This is seen most clearly in Fig. 4 which depicts the temporal evolution of a 1-D  $y-t$  cut through the dotted line shown in Fig. 3(a). Comparing panels (b) and (c) to the true profile in panel (a), it can be seen that only the PARADISE reconstructions captures the correct contraction/expansion pattern of the heart. This is expected since the progressive scheme essentially (and falsely) assumes that the heart is static over a period of  $N_y \cdot TR/R = 352$  ms (with  $R=2$ ) while the PARADISE scheme is designed to account not only for the periodic motion of the heart, but also its beat-to-beat variation.

Note that, in order to achieve the optimum performance with PARADISE, it is essential to consider the coil-sensitivity profiles at both the acquisition design and reconstruction stages (Section 3.2). In other words, one cannot achieve the PARADISE performance gain by simply skipping sampling locations from the  $k-t$  sampling sequence prescribed by PARADIGM. In general, the SNR performance will no longer be optimal and doing so can violate the reconstructability conditions [6]. To demonstrate the importance of optimizing the sampling pattern, we tested a subsampled version of the PARADIGM sampling lattice. The PARADIGM-acquired data [2] was subsampled by a factor of 2 hence achieving a TR of 5.68 ms and the cine was reconstructed using the PARADISE reconstruction scheme. The result is shown in Fig. 3(d). As is seen from the figure, the SNR performance of the subsampled PARADIGM scheme is highly suboptimal. This can also be understood considering that the average spatio-temporal g-factor for this scheme is 6.68 (range: 1.33–8.72) whereas for PARADISE it is 2.11 (range: 1–2.92).

Figure 5 further demonstrates the aforementioned points by depicting the normalized root mean square (RMS) error for the discussed schemes as a function of time. Note that although the progressive scheme achieves low error at times, it is unable of reconstructing the correct object at most times. In case of PARADISE, the error is almost purely due to the additive noise amplification since PARADISE guarantees perfect reconstruction of the signal within the modeled DKT support (which captures 95% of the total energy). This noise amplification is significantly worse in case of the subsampled PARADIGM scheme.

In conclusion, the results indicate that PARADISE is an effective CMRI technique which acquires and reconstructs a full cine with high spatial and temporal resolutions by optimally combining accelerations gained by (i) patient-adaptive imaging and, (ii) parallel imaging, hence achieving accelerations higher than either of (i) or (ii) individually.

## Acknowledgments

This work was partially supported by a graduate fellowship from the Computation Science and Engineering program at the University of Illinois.

## References

1. Zhao, Qi; Aggarwal, Nitin; Bresler, Yoram. Dynamic imaging of time-varying objects. Proc of ISMRM. 2001:1776.
2. Aggarwal, Nitin; Zhao, Qi; Bresler, Yoram. Spatio-temporal modeling and minimum redundancy adaptive acquisition in dynamic MRI. Proc. IEEE ISBI; July 2002; p. 737-740.
3. Bresler, Yoram. Fast acquisition and sampling in MRI: Introduction to time-sequential sampling of spatio-temporal signals. Proc. ISBI; July 2002; p. 713-716.
4. Willis NP, Bresler Y. Lattice-theoretic analysis of time-sequential sampling of spatio-temporal signals - Part I. IEEE Trans Information Theory. Jan.1997 :190–207.
5. Pruessmann KP, et al. SENSE: Sensitivity encoding for fast MRI. Mag Res in Medicine. 1999; 42:952–962.
6. Sharif, Behzad; Bresler, Yoram. Optimal multi-channel time-sequential acquisition in dynamic MRI with parallel coils. Proc. IEEE ISBI; Apr. 2006; p. 45-48.
7. Segars WP, et al. A realistic spline-based dynamic heart phantom. IEEE Trans Nucl Sci. 1999; 46:503–506.
8. Mukkamala R, Cohen RJ. A forward model-based validation of cardiovascular system identification. Am J Physiol. 2001; 281:H2714–H2730.

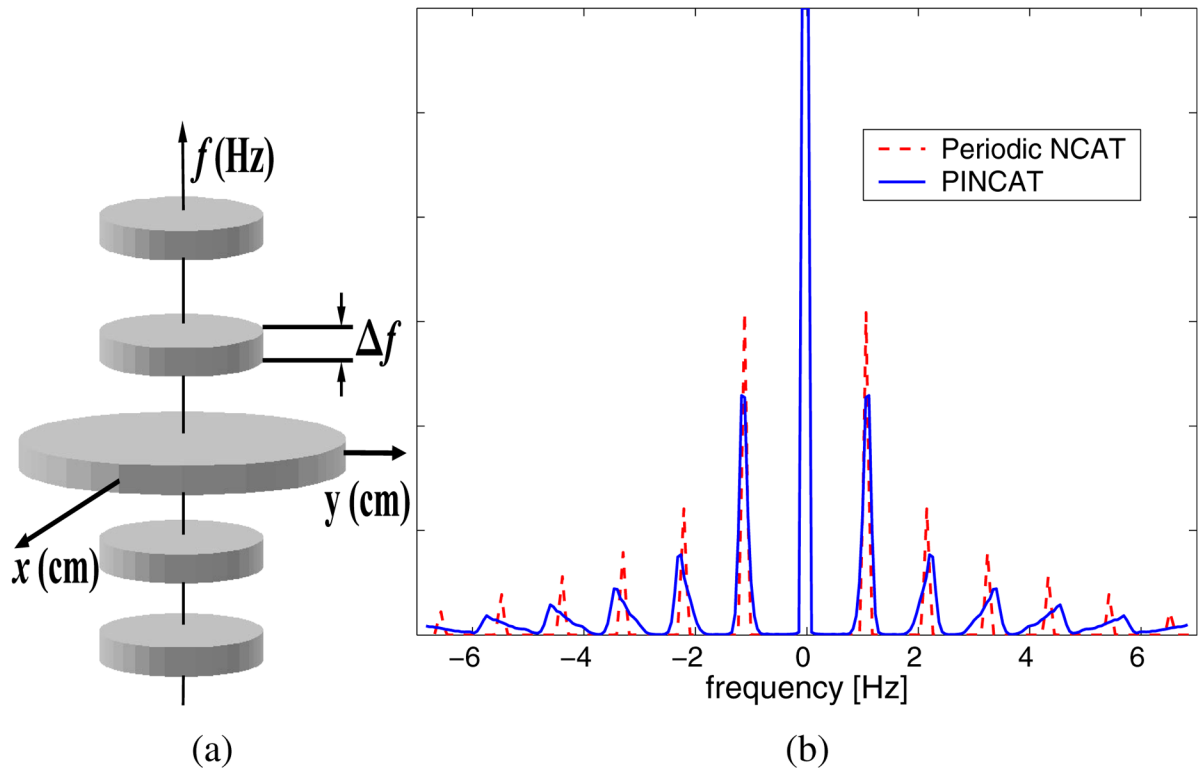


**Fig. 1.**  
The banded spectral DKT model for the heart.



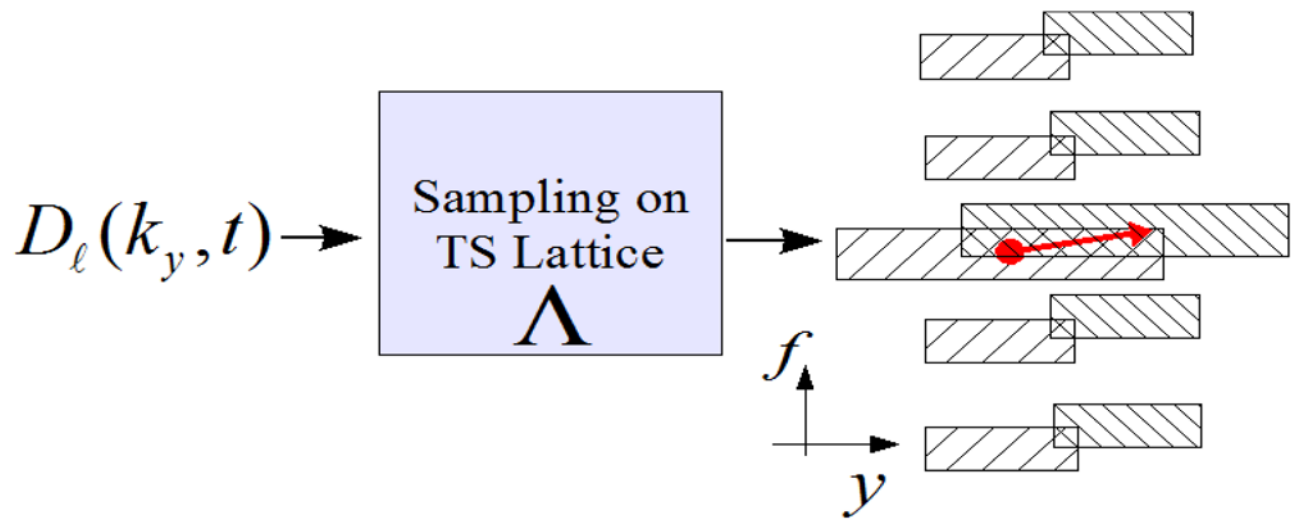


**Fig. 2.** Illustration of the effect of PARADISE sampling in the DKT domain. The arrow marks two members of an EC.

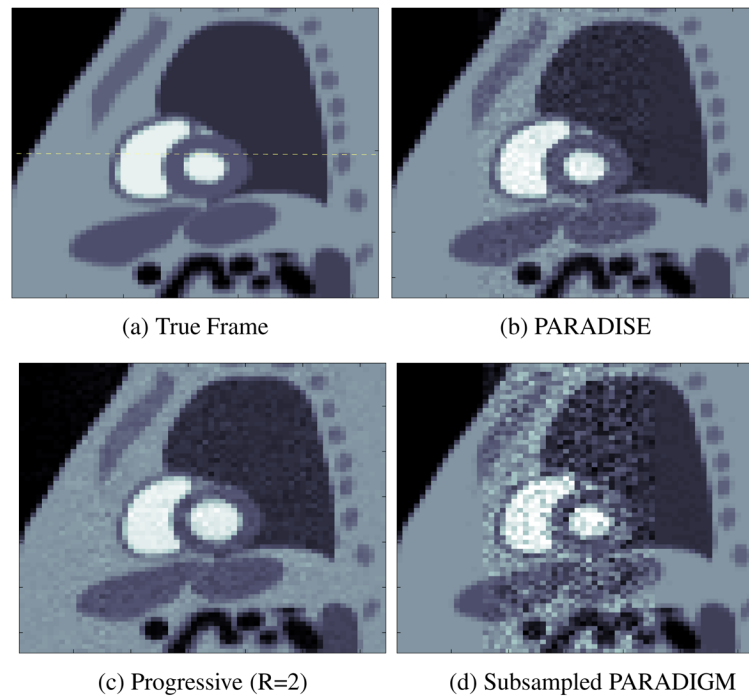
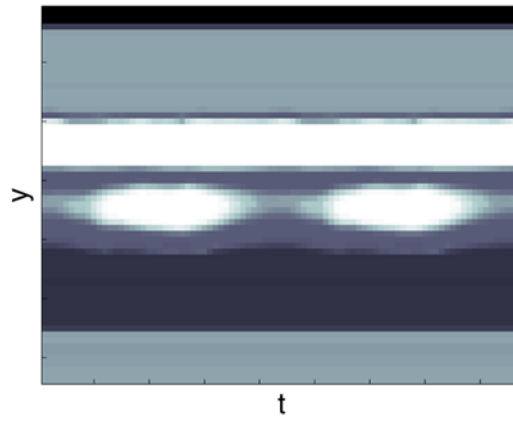
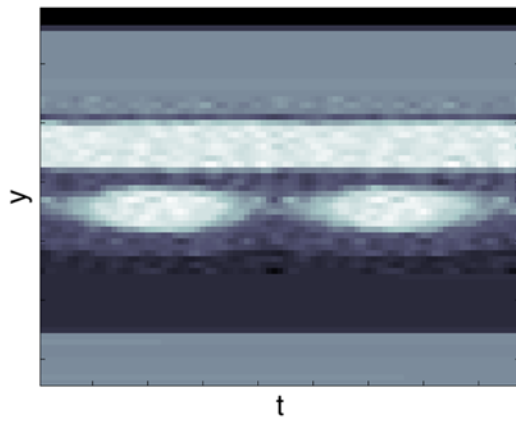


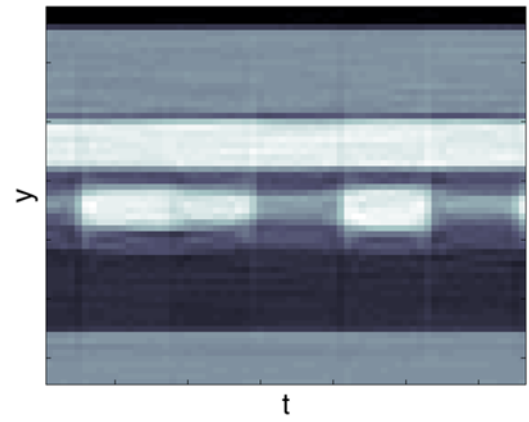
**Fig. 3.** A systolic frame of the reconstructions along with the true frame. The dotted line in (a) marks the location of the cut in Fig. 4.



(a) True profile



(b) PARADISE



(c) Progressive

**Fig. 4.**  
Temporal changes of a  $y$ - $t$  cut through the heart.

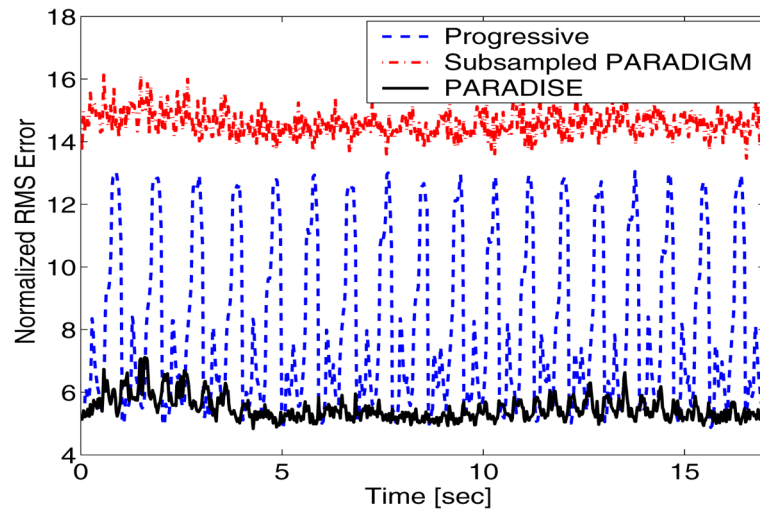


**Fig. 5.**  
Normalized RMS error as a function of time.